

IR Phonon signatures of multiferroicity in TbMn₂O₅

R. Valdés Aguilar,¹ A. B. Sushkov,¹ S. Park,² S-W. Cheong,² and H. D. Drew¹

¹*Materials Research Science and Engineering Center,
University of Maryland, College Park, Maryland 20742*

²*Rutgers Center for Emergent Materials and Department of Physics and Astronomy,
Rutgers University, Piscataway, New Jersey 08854*

The infrared (IR) active phonons in multiferroic TbMn₂O₅ are studied as a function of temperature. Most of the symmetry allowed IR modes polarized along the a and b crystal axes are observed and the behavior of several b polarized phonons is correlated with the magnetic and ferroelectric transitions. A high frequency b polarized phonon only Raman allowed in the paraelectric phase becomes IR active at the ferroelectric transition. The IR strength of this mode is proportional to the square of the ferroelectric order parameter and gives a sensitive measure of the symmetry lowering lattice distortions in the ferroelectric phase.

PACS numbers: 78.30.-j 63.20.Ls 75.50.Ee

I. INTRODUCTION

Materials that exhibit simultaneously (anti)-ferromagnetic, (anti)-ferroelectric or (anti)-ferroelastic degrees of freedom, the so called multiferroics, have become of increasing interest because they offer great possibilities for applications in multifunctional devices. These applications are specially based on the power to control the magnetic state by electric fields and the ferroelectric state by magnetic fields, this type of materials being the magnetoelectrics, a subclass of the multiferroics^{1,2,3,4}. Moreover, the understanding of the basic mechanism that allows this behavior is important in the development of the devices that make use of these characteristics.

The interplay of these degrees of freedom has been demonstrated recently in several multiferroic materials such as $R\text{Mn}_2\text{O}_5$ where R is Eu, Gd, Tb, Dy, Ho and Y^{5,6,7,8,9} as well as in TbMnO_3 ¹⁰ and $\text{Ni}_3\text{V}_2\text{O}_8$ ¹¹. Fundamental questions as to the nature and characteristics of the coupling of the magnetic and ferroelectric orders remain unanswered. Phenomenological approaches^{12,13} based on the Landau theory of phase transitions have been used to relate the symmetry of the spin order with the appearance of ferroelectricity. The basic conclusion of these proposals is that the non-collinearity of the spin system is crucial in the development of ferroelectric order. More microscopic studies^{14,15} have also pointed to the importance of non-collinearity of the spin system.

The antiferromagnetic manganese oxide TbMn₂O₅ (orthorhombic space group Pbam # 55, Z = 4) is a multiferroic with non-collinear magnetic order¹⁶ that shows a strong magnetoelectric coupling effect⁶: an applied magnetic field along the a axis changes the sign of the electrical polarization present along the b axis. The dielectric constant ε along the b axis has anomalies associated with the distinct phase transitions at low temperatures (see figure 1 in Hur, et al⁶): at the Néel temperature $T_N \approx 42$ K no anomalies are present in ε . There is a paraelectric to ferroelectric phase transition at $T_C \approx 38$ K evi-

dent by a peak in the dielectric constant. The magnetic order then locks in to a commensurate structure (CM) with wave vector $(1/2, 0, 1/4)$. At $T \approx 24$ K the magnetic order transforms into an incommensurate structure (ICM) with a step-like feature in ε ; this anomaly is also accompanied by hysteresis⁶. We note that the dielectric constants along the a and c axis show no significant effects at these phase transitions.

In EuMn₂O₅ Polyakov, et al¹⁷ found displacements of the Mn³⁺ ion along the a axis at the ferroelectric transition. They suggested that this behavior leads to a change in symmetry from the space group Pbam to the non-centrosymmetric group P2₁am (# 26). In an analogous work on the compound YMn₂O₅¹⁸, Kagomiya, et al proposed similar displacements at the ferroelectric transition. The displacements reported are very small (≈ 0.007 Å), which hints to a different origin of the ferroelectricity when compared to the typical proper ferroelectrics. Other structural works^{16,19,20} have not reported any signature of atomic displacements at the ferroelectric phase transition in this family of compounds. Moreover, Mikhailova, et al²¹ reported a Raman study in HoMn₂O₅ and TbMn₂O₅ and García-Flores, et al²² in BiMn₂O₅, EuMn₂O₅ and DyMn₂O₅ as a function of temperature and found no evidence of anomalous behavior of the Raman active phonons at the ferroelectric transition temperature. Nevertheless, the existence of a macroscopic dipole moment is evidence of the lack of inversion symmetry in the FE phase, and motivates the study of the dynamics of the lattice to look for further information about the structural changes.

In this report we present a study of the temperature dependent infrared (IR) phonon spectra of the multiferroic TbMn₂O₅. The most interesting feature we find is the appearance of an IR inactive phonon activated at the ferroelectric transition with light polarization parallel to the static ferroelectric polarization \mathbf{P}_0 ($E_\omega || \mathbf{P}_0 || b$). This indicates that one IR forbidden mode (Raman or silent) in the paraelectric phase acquires an electric-dipole moment due to the static displacement associated with the ferroelectricity. We identify this phonon with a Raman

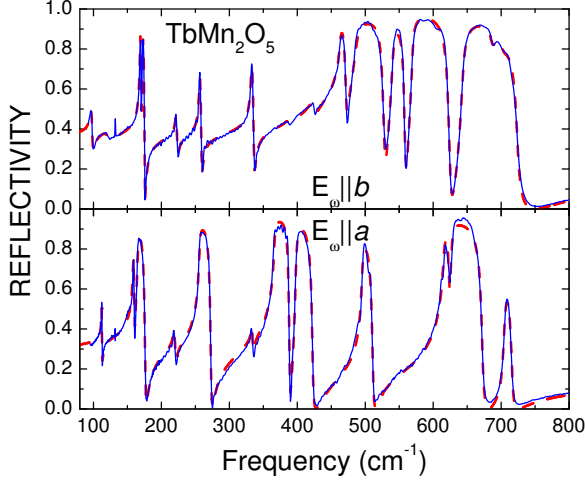


FIG. 1: (Color online). Experimental (solid line) and fit (dashed line) at $T = 7$ K phonon spectra in TbMn_2O_5 .

Mn-O stretching mode, which accounts for its sensitivity to the static polarization possibly induced by the Mn spin system.^{12,20}

II. EXPERIMENTAL RESULTS

Single crystals of TbMn_2O_5 were grown using $\text{B}_2\text{O}_3/\text{PbO}/\text{PbF}_2$ flux in a Pt crucible. The flux was held at 1,280 °C for 15 hours and slowly cooled down to 950 °C at a rate of 1 °C per hour. Crystals grew in the form of black platelets as well as cubes with a typical size of 10 mm³ with a working diameter of 5 mm. The crystals were characterized and oriented using x-ray diffraction at room temperature. Normal incidence reflection spectra were taken with a Bomem Fourier Transform Spectrometer DA3.02. Light was polarized along the a and b crystal axes in the frequency range 8-800 cm⁻¹ (\approx 1-100 meV) and in the temperature range 7 to 300 K. Sample was kept in vacuum in a continuous He flow cryostat with optical access windows. The factor group analysis based on structural data by Alonso, et al²³ of the paraelectric phase gives the following IR active vibrational modes at the Γ point: $\Gamma_{IR} = 8B_{1u}(E||z) + 14B_{2u}(E||y) + 14B_{3u}(E||x)$ identical to a previous report²¹. We complemented this analysis with a shell model calculation of the phonon dispersion.

Figure 1 shows the spectra at $T = 7$ K. Twelve of the 14 IR active phonons in the a polarization were reliably observed, whereas all 14 phonons polarized along b are present in the spectrum. The reflectivity spectra was fitted in a least squares procedure using the sum of Lorentzian form of the model dielectric function ϵ , given

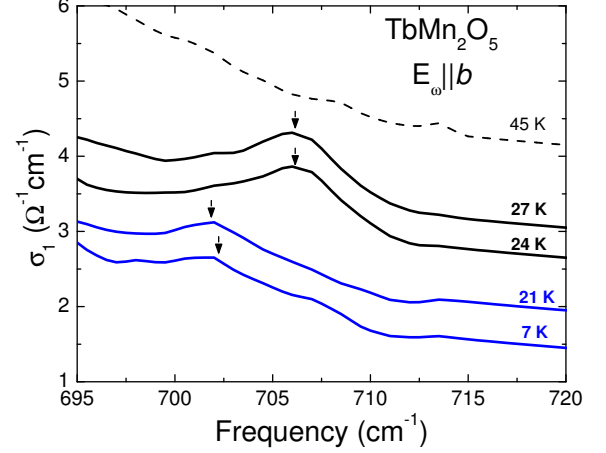


FIG. 2: (Color online). Optical conductivity of the newly activated phonon (shifted plots). Arrows indicate the position of the resonance frequency.

by:

$$\epsilon(\omega) = \epsilon_\infty + \sum_{i=1}^N \frac{S_i}{\omega_{0i}^2 - \omega^2 - i\gamma_i\omega} \quad (1)$$

where ϵ_∞ is the dielectric constant at high frequency and the phonon parameters ω_0 , S and γ are the phonon frequency, the spectral weight and the linewidth respectively, we also define $S_i = \Delta\epsilon_i\omega_{0i}^2$ where $\Delta\epsilon$ is the contribution of the phonon to the static dielectric function; these parameters are extracted as functions of temper-

TABLE I: Oscillator parameters at $T_1 = 7$ K and $T_2 = 45$ K in TbMn_2O_5 . a , b are the crystal axes. $\epsilon_\infty^{a,b} = 5.31, 6.82$.

$\omega_0(\text{cm}^{-1})$				$\Delta\epsilon$				$\gamma(\text{cm}^{-1})$			
a		b		a		b		a		b	
T_1	T_2	T_1	T_2	T_1	T_2	T_1	T_2	T_1	T_2	T_1	T_2
111.9	111.7	97.2	96.4	0.59	0.66	0.42	0.38	1.9	2	3.3	3.7
157.5	157.3	168.9	168.6	0.81	1.05	0.46	0.43	0.9	0.3	1	1.1
164.2	163.8	171.9	171.5	1.68	2.02	0.30	0.35	3.3	2.6	1.4	1.5
218.5	217.4	222.2	221.9	0.30	0.69	0.11	0.11	4.7	8.9	2.4	2.9
254.8	253.2	256.8	256.6	1.88	2.56	0.17	0.18	3.1	1.5	2.1	2
333.1	332.4	333.4	332.7	0.09	0.15	0.17	0.17	2.7	2.6	2.7	2.7
364.9	362.8	386	385.5	2.02	2.75	0.02	0.01	3.9	1	3.5	4
397.6	396.5	422.3	422.3	0.38	0.46	0.28	0.28	4.6	3.2	4	3.5
494.8	493.9	453.2	459.3	0.45	0.59	3.43	3.56	5.3	3.7	18.4	6.7
613.5	611.3	481.8	483	0.71	1.11	2.86	2.6	9	5.4	4.4	3.3
627.5	625.9	538.2	537.6	0.23	0.14	0.25	0.51	8.4	4.2	7.3	7.1
704.2	701.4	567.3	568.4	0.05	0.04	0.52	0.57	3.3	4.5	5.1	7.9
—	—	636.6	637.2	—	—	0.27	0.23	—	—	10.7	9.3
—	—	688.2	686.9	—	—	0.003	0.003	—	—	9.5	6
—	—	703 ^a	—	—	—	0.001	—	—	—	7	—
—	—	120.4 ^b	119.5	—	—	0.12	0.10	—	—	5.7	6.4

^aPreviously IR inactive

^bCrystal field excitation fitted as electric dipole active

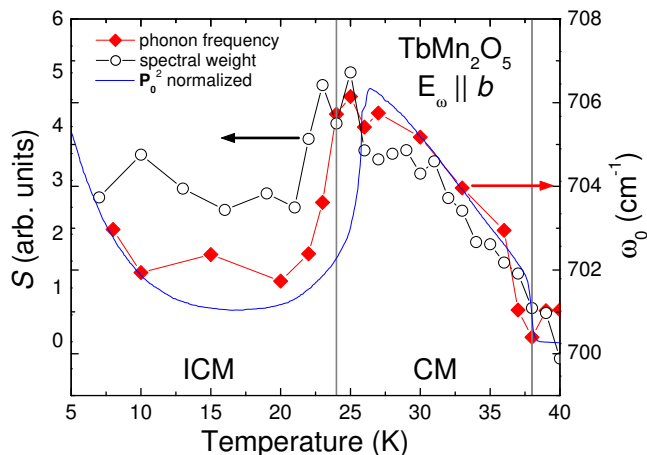


FIG. 3: (Color online). Comparison of the behavior of the spectral weight and frequency of the new phonon to the static polarization \mathbf{P}_0 . Polarization and frequency show warming curves and S shows the cooling curve.

ature and are displayed in table I. The result of the fitting is also shown in figure 1 and it can be seen that it is almost indistinguishable from the data indicating the weakness of higher order phonon processes.

We obtained the optical conductivity using the Kramers-Kronig transform of the reflectivity spectrum. Figure 2 shows the optical conductivity around 700 cm^{-1} for several temperatures with $E_\omega \parallel \mathbf{P}_0$. We observe that a feature not present at 45 K appears in the low T phases. The temperature dependence of the spectral weight and frequency of this feature are plotted in figure 3 where we see the spectral weight starting to appear at 38 K. S for this phonon was obtained by directly integrating the optical conductivity between 695 and 710 cm^{-1} . The spectral weight of this phonon increases and its frequency shifts, both continuously, as we lower the temperature. Around 24 K both abruptly change and show hysteresis around this point evident by the difference in the cooling and warming curves. The behavior of this feature is correlated with the second order FE transition at 38 K and the first order CM \rightarrow ICM transition at 24 K in this compound. The static polarization \mathbf{P}_0 plotted in figure 3 was obtained by measuring the temperature dependence of the pyroelectric current on a similar sample to the one used in the optical measurements.

On very general grounds we can relate the appearance and behavior of this phonon to these underlying phase transitions. Since the lattice distortions δu associated with these phase transitions are very small we can expand the spectral weight and frequency shifts in powers of δu . The quadratic term is the first non-zero term in this expansion that can describe the spectral weight change or frequency shift. Similarly, the order parameters associated with the new phases are proportional to δu so that $\mathbf{P}_0 \propto \delta u$. As a result we expect that the

TABLE II: Irreducible representation splitting at the FE phase transition. S. A. = Spectral Activity (R = Raman active, IR = Infrared Active).

# 55 S. A.	# 55 irreps	# 26 irreps	#26 S. A. ^a
R	A_g	A_1	IR (y) & R
R	B_{1g}	B_2	IR (x) & R
R	B_{2g}	A_2	R
R	B_{3g}	B_1	IR (z) & R
Silent	A_u	A_2	R
IR(z)	B_{1u}	B_1	IR (z) & R
IR(y)	B_{2u}	A_1	IR (y) & R
IR(x)	B_{3u}	B_2	IR (x) & R

^aNote that in this column x, y, z correspond to the high temperature system of coordinates a , b , c and differ from what is found in the character table.

spectral weight behavior and frequency shift should be $S, \Delta\omega \propto (\delta u)^2 \propto \mathbf{P}_0^2$. This is the observed behavior as can be seen in figure 3 where we have plotted \mathbf{P}_0^2 with the phonon data. At low temperatures ($T < 10 \text{ K}$) where the Tb moment orders, the phonon data deviates from \mathbf{P}_0^2 suggesting that it is the Mn and oxygen ion displacements that dominate the dynamics of this high frequency phonon. The possible scenarios for the appearance of a new phonon are: (1) zone folding of the phonon dispersion (since the magnetic order corresponds to a lock in ICM \rightarrow CM transition with $\mathbf{k} = (1/2, 0, 1/4)$), and (2) activation of IR-inactive phonons at this transition due to the loss of inversion symmetry. Our shell model calculation shows that the dispersion of the high frequency phonon is negative so that no zone-folded mode can give the high frequency of this phonon. We therefore conclude that this phonon is a previously IR inactive phonon that acquires electric dipole moment at the FE transition.

In a ferroelectric phase transition, where inversion symmetry is lost, symmetry considerations dictate that phonons that were not IR active in the paraelectric phase can become IR active in the FE phase. This is the case in TbMn_2O_5 , where the low T phase has mixed IR and Raman phonons. In this low T phase the phonons of the high T symmetry group split as shown in table II²⁴. This splitting was obtained by considering what symmetry operation is maintained in both phases and then assign spectral activity according to the experimental observations. The assumption was made as well that the low T space group is as proposed by Polyakov, et al¹⁷ and Kagomiya, et al¹⁸. Consistency with the laboratory frame ($x \rightarrow a, y \rightarrow b, z \rightarrow c$) is applied as well. From the reports by Mihailova, et al.²¹ and García-Flores, et al.²² we learn that a A_g mode at frequency $\approx 700 \text{ cm}^{-1}$ exists in all the RMn_2O_5 materials whose Raman phonons have been reported. We note as well that these reports do not resolve any IR phonons becoming Raman active at the FE phase transition. We conclude that this high frequency A_g Raman phonon is the mode we observe that

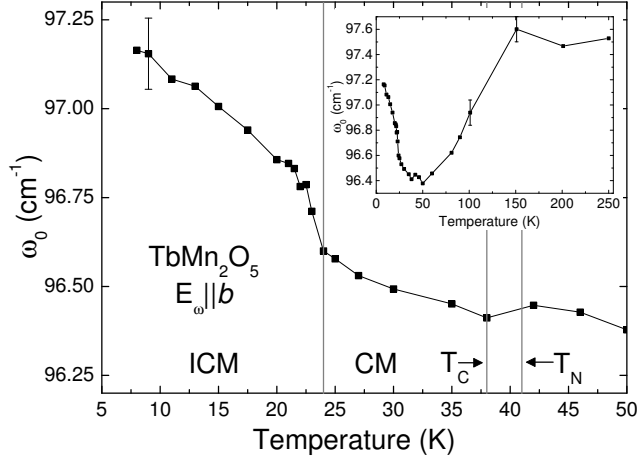


FIG. 4: Temperature dependence of the b axis Tb phonon frequency. Inset shows the full temperature dependence. Typical dispersion of several measurements is indicated as error bars.

acquires IR activity in the FE phase. Further experimental confirmation in the Raman spectrum is needed to make a definitive identification.

Only a few other phonons show correlations with the low temperature phase transitions. The phonons polarized along the a axis do not show any significant anomalies in this temperature range. This is consistent with the featureless behavior of the dielectric function along this axis. On the other hand, the behavior of some of the phonons with dipole moment along b is non-trivial. The low frequency phonon with frequency $\approx 96 \text{ cm}^{-1}$, identified primarily with movement of the Tb ions, has a temperature dependence that correlates with the low temperature CM \rightarrow ICM magnetic transition. In figure 4 the frequency of this phonon is plotted versus temperature and we observe an increase in the frequency around 24 K. This effect is thought to be a manifestation of the coupling of this phonon to a magnon as is discussed by Katsura, et al²⁵. Further experimental results on this effect will be presented elsewhere²⁶.

Surprisingly several phonons show interesting temperature dependence for T above T_N . The inset in figure 4 shows the full temperature dependence of the frequency of the b axis phonon. The anomalous softening in the temperature range of 150 K to 50 K demonstrates additional effects in the dynamics of the lattice. In figure 5 the behavior of the spectral weight of two oxygen phonons polarized in the a and b axes, with frequencies of 704 and 689 cm^{-1} respectively, seems complementary: the a phonon gains spectral weight while the b phonon loses it as the temperature is lowered. This effect is present in the full temperature range from 300 K to 7 K, while for the rest of the phonons the spectral weight is only changed significantly around the various transition temperatures. The fact that these modes gain or lose so much spectral

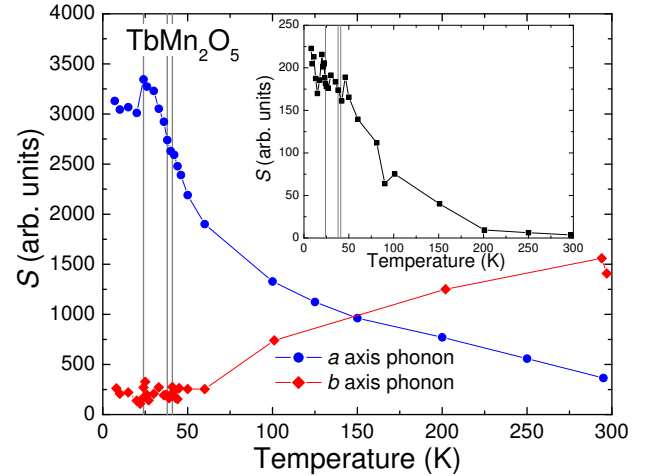


FIG. 5: (Color online). Temperature dependence of the spectral weight of 2 oxygen dominated phonons. Inset shows the temperature dependence of the spectral weight of one of the Tb^{3+} crystal field transitions.

weight (10 and 6-fold respectively) in a large temperature interval also demonstrates some higher energy scale in this system. These effects (the anomalous softening and the dramatic changes in spectral weight) are not understood at present. However, one interesting possibility is that they are of magnetic character. Recent high temperature susceptibility measurements²² in BiMn_2O_5 has shown evidence for spin frustrated behavior from deviations from Curie law with a Weiss temperature of $\approx 250 \text{ K}$. Dielectric anomalies in BiMn_2O_5 around this temperature have been reported²⁷ as well.

Finally the inset of figure 5 shows the temperature dependence of the intensity of a feature observed at 120 cm^{-1} . This is identified as a crystal field level of the Tb^{3+} ion²⁸. This transition has electric dipole character as is seen from the form of the reflectivity curve (see fig. 1) as well as the fact that the spectral weight (see table I) is comparable to the IR active phonons (magnetic dipole transitions are usually much weaker than electric dipole transitions). This conclusion is supported as well by the shell model calculation that shows the 3 lowest phonon excitations being the Tb-dominated phonon (at $\approx 100 \text{ cm}^{-1}$) and then a doublet (at $\approx 170 \text{ cm}^{-1}$). Furthermore, the observed temperature dependence of the intensity is common for the f-level crystal field transitions in the rare earth ions²⁹. Several other absorption features are observed in transmission at lower frequencies and will be reported elsewhere²⁶.

III. CONCLUSIONS

We have measured the IR phonon spectra in TbMn_2O_5 along the a and b axes and have observed most of the symmetry allowed modes. The majority of the phonons

do not show significant correlations to the FE and AFM phase transitions of the system. However several phonons exhibit interesting correlations to the ferroelectricity of this material. We have found a signature of the loss of inversion symmetry in the FE phase by the appearance of a IR phonon below T_c that was only Raman active in the paraelectric phase. The strength of this mode is proportional to the square of the FE order parameter and gives a sensitive measure of the symmetry lowering lattice distortions in the ferroelectric phase. In addition, the lowest frequency phonon (along b) displays hardening in the CM \rightarrow ICM transition possibly due to the coupling with the spin system²⁵; 2 modes (along a and b) have dramatic changes in their spectral weight over a wide

temperature range possibly because of frustration effects in the spin system. We have also identified an electric dipole active crystal field transition of the Tb^{3+} ion in the phonon frequency range.

IV. ACKNOWLEDGEMENTS

We thank G-W. Chern, D.I. Khomskii, S. Jandl, J. Simpson and O. Tchernyshyov for useful discussions. This work was supported by the National Science Foundation MRSEC under Grant No. DMR-0520471.

-
- ¹ N. A. Hill and A. Filippetti, *J. Mag. Mag. Mat.* **242-245**, 976 (2002).
 - ² M. Fiebig, T. Lottermoser, T. Lonkai, A. V. Goltsev, and R. V. Pisarev, *J. Mag. Mag. Mat.* **290-291**, 883 (2005).
 - ³ W. Prellier, M. P. Singh, and P. Murugavel, *J. Phys. Condens. Matter* **17**, R803 (2005).
 - ⁴ C. Binek and B. Doudin, *J. Phys. Condens. Matter* **17**, L39 (2005).
 - ⁵ Y. F. Popov, A. M. Kadomtseva, S. S. Krotov, G. P. Vorob'ev, and M. M. Lukina, *Ferroelectrics* **279**, 147 (2002).
 - ⁶ N. Hur, S. Park, P. Sharma, J. Ahn, S. Guha, and S.-W. Cheong, *Nature* **429**, 392 (2004).
 - ⁷ N. Hur, S. Park, P. A. Sharma, S. Guha, and S.-W. Cheong, *Phys. Rev. Lett.* **93**, 107207 (2004).
 - ⁸ E. Golovenchits and V. Sanina, *J. Phys. Condens. Matter* **16**, 4325 (2004).
 - ⁹ D. Higashiyama, S. Miyasaka, N. Kida, T. Arima, and Y. Tokura, *Phys. Rev. B* **70**, 174405 (2004).
 - ¹⁰ T. Kimura, T. Goto, H. Shintani, K. Ishizaka, T. Arima, and Y. Tokura, *Nature* **426**, 55 (2003).
 - ¹¹ G. Lawes, A. B. Harris, T. Kimura, N. Rogado, R. J. Cava, A. Aharony, O. Entin-Wohlman, T. Yildirim, M. Kenzelmann, C. Broholm, et al., *Phys. Rev. Lett.* **95**, 087205 (2005).
 - ¹² M. Mostovoy, *Phys. Rev. Lett.* **96**, 067601 (2006).
 - ¹³ A. B. Harris (2005), *CondMat/0508730*.
 - ¹⁴ H. Katsura, N. Nagaosa, and A. V. Balatsky, *Phys. Rev. Lett.* **95**, 057205 (2005).
 - ¹⁵ I. A. Sergienko and E. Dagotto, *Phys. Rev. B* **73**, 094434 (2006).
 - ¹⁶ L. C. Chapon, G. R. Blake, M. J. Gutmann, S. Park, N. Hur, P. G. Radaelli, and S.-W. Cheong, *Phys. Rev. Lett.* **93**, 177402 (2004).
 - ¹⁷ V. Polyakov, V. Plakhty, M. Bonnet, P. Burlet, L.-P. Regnault, S. Gavrilov, I. Zobkalo, and O. Smirnov, *Physica B* **297**, 208 (2001).
 - ¹⁸ I. Kagomiya, S. Matsumoto, K. Kohn, Y. Fukuda, T. Shoubu, H. Kimura, Y. Noda, and N. Ikeda, *Ferroelectrics* **286**, 167 (2002).
 - ¹⁹ G. R. Blake, L. C. Chapon, P. G. Radaelli, S. Park, N. Hur, S.-W. Cheong, and J. Rodríguez-Carvajal, *Phys. Rev. B* **71**, 214402 (2005).
 - ²⁰ L. C. Chapon, P. G. Radaelli, G. R. Blake, S. Park, and S.-W. Cheong, *Phys. Rev. Lett.* **96**, 097601 (2006).
 - ²¹ B. Mihailova, M. M. Gospodinov, B. Guttler, F. Yen, A. P. Litvinchuk, and M. N. Iliev, *Phys. Rev. B* **71**, 172301 (2005).
 - ²² A. F. García-Flores, E. Granado, H. Martinho, R. R. Urbano, C. Rettori, E. I. Golovenchits, V. A. Sanina, S. B. Oseroff, S. Park, and S.-W. Cheong, *Phys. Rev. B* **73**, 104411 (2006).
 - ²³ J. Alonso, M. Casais, M. Martínez-Lope, J. Martínez, and M. Fernández-Díaz, *J. Phys. Condens. Matter* **9**, 8515 (1997).
 - ²⁴ The exact space group for the FE phase in TbMn_2O_5 is not known precisely. We have made the assumption of space group # 26 following Polyakov, et al¹⁷ and Kagomiya, et al¹⁸, because this allows to write the direct transformation of each phonon for both space groups. Nevertheless, even if the real crystallographic structure is different, such as the modulated structure in DyMn_2O_5 ⁹, our experimental observation and analysis would not change.
 - ²⁵ H. Katsura, A. V. Balatsky, and N. Nagaosa (2006), *CondMat/0602547*.
 - ²⁶ A. B. Sushkov, R. Valdés Aguilar, S.-W. Cheong, S. Park, and H. D. Drew, unpublished.
 - ²⁷ E. I. Golovenchits, V. A. Sanin, and A. V. Babinskiĭ, *JETP* **85**, 156 (1997).
 - ²⁸ M. J. P. Gingras, B. C. den Hertog, M. Faucher, J. S. Gardner, S. R. Dunsiger, L. J. Chang, B. D. Gaulin, N. P. Raju, and J. E. Greedan, *Phys. Rev. B* **62**, 6496 (2000).
 - ²⁹ S. Jandl, private communication (2006).